DOI: 10.1002/ejic.200600960

Synthesis and Sublimation Kinetics of a Highly Volatile Asymmetric Iron(II) Amidinate

Xin-Gui Li,*[a,b] Zhengwen Li,[a] Huazhi Li,[a] and Roy G. Gordon*[a]

Keywords: Asymmetric iron(II) amidinate / Bridging ligands / Metathesis / Sublimation kinetics / Thermochemistry

A highly volatile asymmetric iron(II) amidinate, iron(II) bis(*N*-*tert*-butyl-*N*′-ethylacetamidinate), was synthesized for the first time by systematically changing starting iron(II) compounds such as acetylacetonate, acetate, and chloride, in different media such as diethyl ether, toluene, and tetrahydrofuran. The amidinate has been characterized and compared with the symmetric iron(II) bis(*N*,*N*′-diisopropylacetamidinate) by NMR spectroscopy, MS, IR spectroscopy, and dynamic and isothermal thermogravimetric techniques. Different amidinates from three starting compounds exhibit almost the same NMR, MS, and IR spectra, a melting point of 85 °C, and the same solution color in the same solvents, but quite different synthetic yields, volatilities, and colors in different solvents. This implies that the amidinates show an interesting solvatochromism. In particular, the asymmetric iron(II) amidinates obtained should be a mixture of paramagnetic and diamagnetic compounds. The thermostability and sublimation kinetics of the iron(II) amidinates have been investigated in detail. It is found that the average activation energy of 106 kJ mol^{-1} for the nonisothermal sublimation is slightly higher than the average activation energy of 104 kJ mol^{-1} determined from the isothermal thermogravimetric experiments. The sublimation is a diffusion-controlled process because the temperature and the rate of the sublimation depend strongly on the sublimation level and the sample size. The optimal iron(II) starting compound and reaction medium should be iron(II) acetylacetonate and diethyl ether, respectively, because the combination offers the highest yield, the greatest volatilizability of 98 %, and thus the purest product.

Introduction

Metal amidinate complexes with intriguing structural diversity and novel properties have been the subject of intense investigations in chemistry, electronics, optics, energy, and materials science.[1–4] Great interest has been focused on the applicability of the complexes as single-source precursors of advanced functional materials,[5] efficient homogeneous catalysts in olefin and caprolactone polymerizations,[6–7] initiators for the stereospecific and degenerative transfer living Ziegler–Natta polymerization of alpha-olefins with an extremely high level of stereoselectivity,[8] and activators for the polymerization of *rac*-lactide to produce heterobiased polylactides.[9] Metal-based amidinate complexes that are of particular relevance to this paper have been used as highly volatile precursors for atomic layer deposition of films with novel multifunctionalities and a wide variety of applications in modern high technology, including semiconductor microelectronics, high-resolution displays, optical filters, magnetic information storage, and catalysis.[10–12]

The precursors need to be designed in such a way that the compounds are volatile and thermally stable at growth temperatures.[10,13] Generally, the more volatile the better the precursors are. The synthesis and characterization of numerous metal compounds with amidinate ligands have been reported in the literature.[10,12–14] The volatility and thermal stability of symmetric amidinates of transition metals and lanthanum with oxidation states of one (Cu, Ag, Au),[15] two (Mg, Mn, Fe, Co, Ni),[16] three (Ti, V, Y, Al, Ga, La),[17] and four (Ru, Hf)[8] have been reported. Note that the symmetric metal amidinates usually exhibit a lower volatility than asymmetric metal amidinates with the same molar mass because there is relatively disordered molecular aggregation and hence a lower molecular interaction among the asymmetric amidinates. However, no studies on the synthesis, characterization, and volatility of asymmetric iron(II) amidinates were found to the best of our knowledge.

Herein we describe a facile synthesis of a highly volatile asymmetric iron(II) amidinate, iron(II) bis(*N*-*tert*-butyl-*N*′-ethylacetamidinate). The effect of starting iron(II) compounds and amidination solvents on the synthetic yield, molecular structure, and properties of the iron(II) amidinate was studied. The NMR spectral characteristics of various iron(II) amidinates obtained under different synthetic

[a] Department of Chemistry and Chemical Biology, Harvard University,
12 Oxford Street, Cambridge, MA 02138, USA
Fax: +1-617-495-4723
E-mail: adamxgli@yahoo.com
gordon@chemistry.harvard.edu
[b] Institute of Materials Chemistry, College of Materials Science & Engineering, Tongji University,
1239 Siping Road, Shanghai 200092, China
Fax: +86-21-6598-0524
E-mail: adamxgli@yahoo.com

conditions were carefully compared. In particular, the thermostability, volatility, and sublimation kinetics were investigated in detail for the first time.

Results and Discussion

Synthesis of Iron(II) Amidinates

All iron amidinate compounds listed in Table 1 were synthesized by the metathesis reactions of starting iron compounds with corresponding equivalents of the lithium amidinates [*N*-*tert*-butyl-*N*′-ethylacetamidinate (*t*Bu-Et-MeAMD) and *N*,*N*′-diisopropylacetamidinate (*i*Pr-MeAMD)] in various solvents. Lithium amidinates were prepared in situ from the corresponding carbodiimide with methyllithium and not isolated. Compounds **1**–**3** and **6**–**7** are all solids at room temperature but compounds **4**–**5** look like semisolids at room temperature. The synthetic yield and physical properties are summarized in Table 1. It appears that the starting iron(II) compounds and acetamidination solvents influence the synthesis and properties of the final iron complexes.

In the solvent diethyl ether it is found that the yield increases and product color darkens when changing the starting iron(II) materials from iron(II) acetate to iron(II) chloride to iron(II) acetylacetonate. This phenomenon should be attributed to the solubility difference of the three iron compounds in diethyl ether. Iron(II) acetate is almost insoluble in diethyl ether and iron(II) chloride is slightly soluble in diethyl ether. However, iron(II) acetylacetonate is nearly completely soluble in diethyl ether. As a result the highest yield achieved with iron(II) acetylacetonate as the starting material should be ascribed to its best solubility in diethyl ether. Note that the three iron amidinate products obtained have similar melting points and sublimation temperatures.

In addition, the synthetic yield increases steadily when changing the acetamidination solvent from toluene to THF to diethyl ether by using a fixed starting iron(II) material of iron(II) acetylacetonate, which could result from an increased solubility of iron(II) acetylacetonate in toluene to THF to diethyl ether. The product obtained in THF has the lowest melting point. A similar variation of the yield and melting point with changing solvent from THF to diethyl ether is observed with a fixed starting iron(II) material of iron(II) chloride. It can then be concluded that a combination of iron(II) acetylacetonate and diethyl ether is better for the synthesis of the asymmetric iron(II) bis(*N*-*tert*-butyl-*N*′-ethylacetamidinate)s giving a higher yield. On the contrary, this combination produces a symmetric iron(II) bis(*N*,*N*′-diisopropylacetamidinate) with a lower yield but higher melting point than the asymmetric iron(II) bis(*N*-*tert*-butyl-*N*′-ethylacetamidinate)s. The different colors of the final solid products could be ascribed to different spatial arrangements of atoms from different starting materials or acetamidination solvents regardless of their same molecular structure.

Molecular Structure of the Iron(II) Amidinates

The asymmetric iron(II) amidinates were systematically characterized by ^{1}H NMR, IR and MS methods. It seems that the NMR spectra of the compounds do not display a high resolution, possibly because of the presence of a very small amount of impurity resulting from their light sensitivity. Just like other paramagnetic iron(II) amidinates,[18,19] however, the ^{1}H NMR spectra of the asymmetric iron(II) amidinates in $CDCl_3$ show two series of resonance peaks over a very wide chemical shift range from –10 to +200 ppm. The first series of resonance peaks at 8.6 ppm (sharp, NCH_2CH_3), 3.5 ppm (sharp, N_2CCH_3), 1.5 ppm [broad, $NC(CH_3)_3$], and 0.3 ppm (sharp triplet, NCH_2CH_3) are typically attributed to the diamagnetic fraction. The second series of resonance peaks at δ = 199.5 ppm (broad, NCH_2CH_3), 56.7–111 ppm (sharp, N_2CCH_3), 29.7 ppm [broad, $NC(CH_3)_3$], and –6.1 ppm (sharp triplet, NCH_2CH_3) are ascribed to the paramagnetic fraction because of their much higher chemical shift. Therefore, the area ratio, calculated from the resonance peaks at 29.7 over 1.5 ppm, could be used to estimate the paramagnetic percentage, as listed in Table 1. As shown in Figure 1, ^{1}H NMR spectra of the iron(II) bis(*N*-*tert*-butyl-*N*′-ethylacetamidinate) in $CDCl_3$ look almost the same regardless of the change of starting iron(II) materials from iron(II) acetate and $FeCl_2$ to iron(II) acetylacetonate for the synthesis of the asymmetric iron(II) amidinate. This implies that the three iron(II) amidinates that were obtained should have

Table 1. The synthesis and principal parameters of the iron(II) bis(*N*-*tert*-butyl-*N*′-ethylacetamidinate)s and bis(*N*,*N*′-diisopropylacetamidinate).

No.	Acetamidination conditions Starting materials			Solvent	Iron(II) bis(*N*-*tert*-butyl-*N*′-ethylacetamidinate)s Yield	Color of the solid obtained	M.p.	Paramagnetic fraction in $CDCl_3$	Subl. temp. at 10 °C min^{-1}
					[%]		[°C]	[mol.-%]	[°C]
1	[a]	MeLi	iron(II) acetate	diethyl ether	22	purplish blue	85	60	141
2	[a]	MeLi	iron(II) chloride	diethyl ether	25	dark blue	85	58	140
3	[a]	MeLi	iron(II) acetylacetonate	diethyl ether	42	black	85	55	147
4	[a]	MeLi	iron(II) acetylacetonate	THF	22	reddish black	30	47	141
5	[a]	MeLi	iron(II) chloride	THF	7	dark black	30	54	–
6	[a]	MeLi	iron(II) acetylacetonate	toluene	11	purplish black	85	37	177
7	[b]	MeLi	iron(II) acetylacetonate	diethyl ether	22	dark blue	95	–	130

[a] 1-*tert*-Butyl-3-ethylcarbodiimide. [b] 1,3-Diisopropylcarbodiimide.

the same molecular structure. Note that their paramagnetic percentages and sublimation behavior (as discussed below) are slightly different. It is seen from Table 1 that the highest paramagnetic percentage, up to 60%, could be found in the amidinate made from iron(II) acetate.

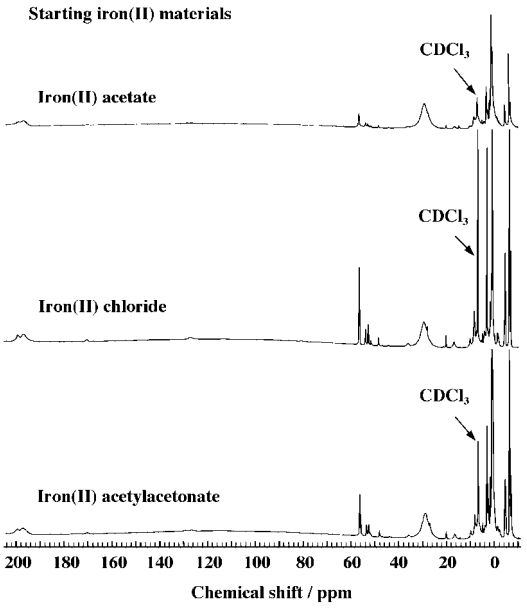

Figure 1. The ^{1}H NMR spectra of the resulting iron(II) bis(*N*-*tert*-butyl-*N*′-ethylacetamidinate)s obtained with iron(II) acetate, chloride, and acetylacetonate as starting iron(II) materials, respectively.

However, the ^{1}H NMR spectra of the iron(II) bis(*N*-*tert*-butyl-*N*′-ethylacetamidinate) vary significantly with the amidination media and NMR testing solvent used in the synthesis of the iron(II) amidinates, regardless of whether the other conditions are kept constant, as shown in Figure 2 and Figure 3. It is found from Figure 2 that the iron(II) bis(*N*-*tert*-butyl-*N*′-ethylacetamidinate) obtained in diethyl ether exhibits nearly the same ^{1}H NMR spectral characteristics as that obtained in THF, signifying that the molecular structure of the iron(II) bis(*N*-*tert*-butyl-*N*′-ethylacetamidinate)s obtained in diethyl ether and THF should be very similar. Note that the iron(II) bis(*N*-*tert*-butyl-*N*′-ethylacetamidinate) obtained in toluene displays quite a different spectrum with a chemical shift range of 10–205 ppm compared with those obtained in diethyl ether and THF. In addition, their paramagnetic percentages and sublimation behavior (as discussed below) are distinctly different. Table 1 reveals that the paramagnetic percentage in the iron(II) bis(*N*-*tert*-butyl-*N*′-ethylacetamidinate) obtained from the same iron(II) acetylacetonate consistently increases from 37 to 47 to 55% when changing the amidination solvent from toluene to THF to diethyl ether. A similar situation is also discovered for the iron(II) bis(*N*-*tert*-butyl-*N*′-ethylacetamidinate) obtained from the same $FeCl_2$. This structure difference might be attributable to the different structural characteristics of the solvents used. Toluene is an aromatic hydrocarbon with a low dielectric constant (2.3), whereas diethyl ether and THF are aliphatic ether solvents with relatively high dielectric constants (4.2 and 7.4, respectively). That is to say, acetamidination solvents will significantly influence the synthesis of the target iron(II) bis(*N*-*tert*-butyl-*N*′-ethylacetamidinate), notwithstanding the other conditions. Hence, the acetamidination solvents should be carefully selected for the synthesis of an ideal asymmetric iron(II) amidinate. The ether could be an optimal acetamidination solvent for the synthesis of the iron(II) bis(*N*-*tert*-butyl-*N*′-ethylacetamidinate).

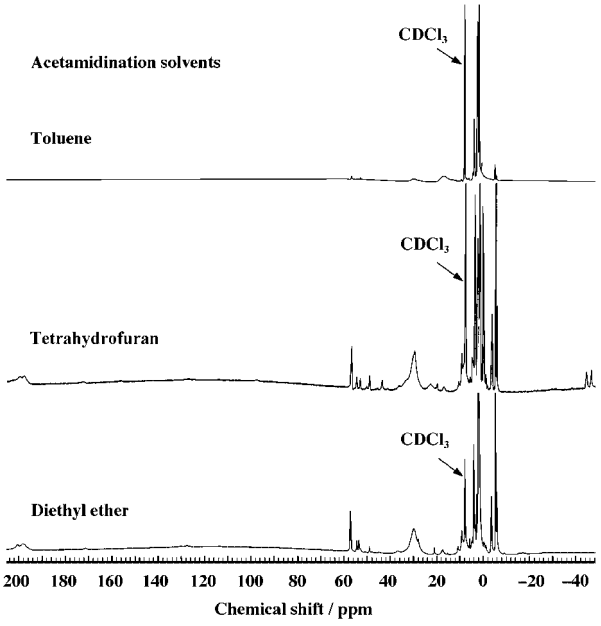

Figure 2. The effect of the acetamidination solvent on the ^{1}H NMR spectra of the iron(II) bis(*N*-*tert*-butyl-*N*′-ethylacetamidinate)s with iron(II) acetylacetonate as the same starting iron(II) material.

Figure 3 reveals that the same iron(II) bis(*N*-*tert*-butyl-*N*′-ethylacetamidinate) obtained in diethyl ether exhibits totally different NMR spectra if NMR testing solvents were changed from C_6D_6 to $CDCl_3$ to C_5D_5N with dielectric constants of 2.3, 4.8, and 13.3, respectively. This should result from different interactions between the iron amidinate and solvent molecules with different characteristics. In particular, the NMR spectrum obtained in C_6D_6 suggests the lowest paramagnetism, whereas the NMR spectrum in C_5D_5N suggests the highest paramagnetic content of up to 60%, implying that the paramagnetism of the iron(II) amidinates depends on the solvent characteristics. It appears that the paramagnetism of the complexes in the solvent with the highest dielectric constant is higher. The diversification of the NMR spectra with changing NMR testing solvents from $CDCl_3$ to C_6D_6 to C_5D_5N is also observed for the same iron(II) bis(*N*,*N*′-diisopropylacetamidinate) in this study. Therefore, NMR testing solvents should be carefully chosen for the obtainment of an ideal NMR spectrum of the paramagnetic materials. The deuterated solvent with a high dielectric constant could be optimal for the NMR spectroscopic analysis.

IR spectra of iron(II) complexes obtained show the expected and very strong absorptions at 1651–1653 and 548 cm^{-1} attributable to the delocalized –N⋯C⋯N– and Fe–

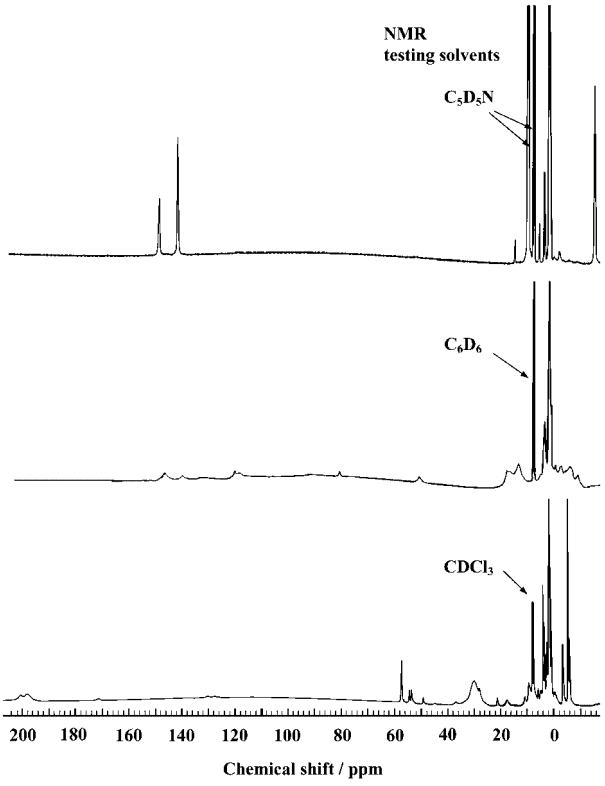

Figure 3. The effect of the NMR testing solvent on the ^{1}H NMR spectra of the same iron(II) bis(*N*-*tert*-butyl-*N*′-ethylacetamidinate) with iron(II) acetylacetonate as a starting iron(II) material in diethyl ether.

N stretching modes, respectively, but no characteristic absorptions at 3436 and 2100 cm^{-1} due to the amidine ϕ_{NH} and free carbodiimide $\upsilon_{N=C=N}$ stretching modes are observed.[20,21] These results strongly suggest the formation of the iron(II) bis(*N*-*tert*-butyl-*N*′-ethylacetamidinate).

In the mass spectra, all the amidinate complexes are characterized by a loss of the methyl and *tert*-butyl groups from the ions.[18] The ligand bonds between N and Fe break the most easily. It seems that the breaking mode of the complexes does not change with elevating MS testing temperatures from 120, 150, to 300 °C. However, the MS spectra indeed vary if 10% water is added to MCN or when changing starting iron(II) materials from acetylacetonate to acetate to chloride. These results also significantly indicate a successful synthesis of the iron(II) bis(*N*-*tert*-butyl-*N*′-ethylacetamidinate).

Sublimation and Volatility of the Iron(II) Amidinates

TG and derivative thermogravimetry (DTG) curves of the iron(II) bis(*N*-*tert*-butyl-*N*′-ethylacetamidinate)s obtained from three starting iron(II) compounds in diethyl ether are given in Figure 4. Sublimation or thermal decomposition occurs clearly in one step at a lower temperature (110–170 °C)[10,13] with a lower residual mass of 3%, that is, a higher volatility of 97%. The low sublimation temperature of iron(II) bis(*N*-*tert*-butyl-*N*′-ethylacetamidinate) might be ascribed to the weak intermolecular forces, which are due to its spherical shape (Scheme 1). The weaker intermolecular forces of iron(II) bis(*N*,*N*′-diisopropylacetamidinate) can also be used to explain the fact that its sublimation temperature (Table 1) is lower than that of the iron(II) bis(*N*-*tert*-butyl-*N*′-ethylacetamidinate), which has the same molecular mass, because the iron(II) bis(*N*,*N*′-diisopropylacetamidinate) molecule should be more spherical and more symmetric. The iron(II) bis(*N*-*tert*-butyl-*N*′-ethylacetamidinate)s obtained with iron(II) acetate and chloride as starting iron(II) materials exhibit the same sublimation or volatile characteristics, which are different from that of the iron(II) bis(*N*-*tert*-butyl-*N*′-ethylacetamidinate) obtained with iron(II) acetylacetonate. The iron(II) bis(*N*-*tert*-butyl-*N*′-ethylacetamidinate) obtained with iron(II) acetylacetonate begins to sublimate at a higher temperature with a further residual weight of 2% lower than the other two. In other words, the iron(II) bis(*N*-*tert*-butyl-*N*′-ethylacetamidinate) obtained with iron(II) acetylacetonate possesses the highest volatilizability of 98%.

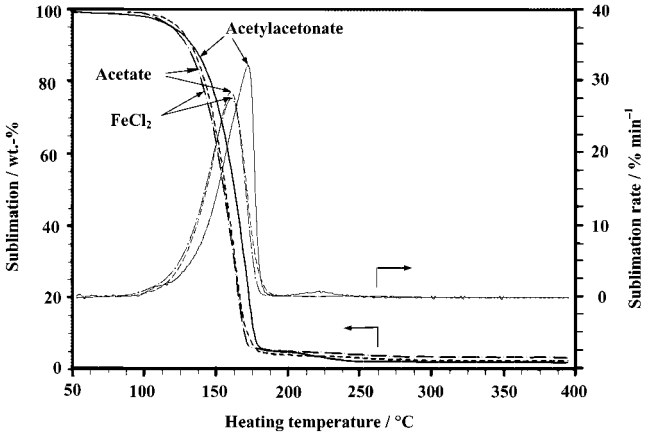

Figure 4. The effect of the starting iron(II) compounds on the sublimation of the iron(II) bis(*N*-*tert*-butyl-*N*′-ethylacetamidinate) obtained in diethyl ether at a heating rate of 10 °C/min.

The TG sublimation thermograms of the iron(II) bis(*N*-*tert*-butyl-*N*′-ethylacetamidinate)s vary significantly with iron(II) amidination solvents despite the same synthetic conditions being used, as shown in Figure 5. It is found that the iron(II) bis(*N*-*tert*-butyl-*N*′-ethylacetamidinate) obtained in diethyl ether exhibits nearly the same major sublimation characteristics as that obtained in THF, suggesting that the two iron(II) bis(*N*-*tert*-butyl-*N*′-ethylacetamidinate)s obtained in diethyl ether and THF should be very similar. However, the iron(II) bis(*N*-*tert*-butyl-*N*′-ethylacetamidinate) obtained in THF displays a much higher residual weight percentage or lower volatilizability than that obtained in diethyl ether, implying that the latter is much purer in composition. Note that the iron(II) bis(*N*-*tert*-butyl-*N*′-ethylacetamidinate) obtained in toluene displays quite a different TG thermogram as compared with those obtained in diethyl ether and THF, indicative of the iron(II) amidinates having different molecular structures. This is corroborated by the NMR results discussed above. The

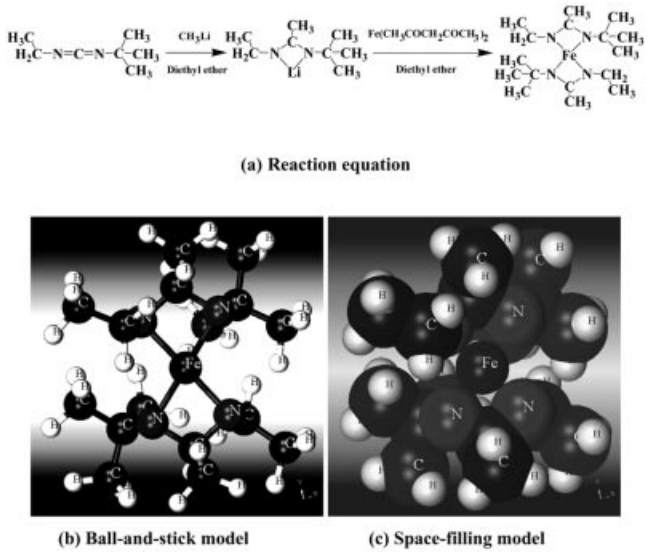

Scheme 1. The synthesis of the iron(II) bis(*N*-*tert*-butyl-*N*′-ethylacetamidinate) and its structural models at the minimum energy.

iron(II) bis(*N*,*N*′-diisopropylacetamidinate) obtained with iron(II) acetylacetonate as the iron(II) source exhibits a much lower sublimation temperature (150 °C) at the maximal-sublimation rate than that (225 °C) of the iron(II) bis(*N*,*N*′-diisopropylacetamidinate) obtained with $FeCl_2$ as the iron(II) source.[10] This suggests that iron(II) acetylacetonate could be a better starting iron(II) material for the synthesis of the iron(II) amidinates with higher volatility at a much lower temperature than $FeCl_2$.

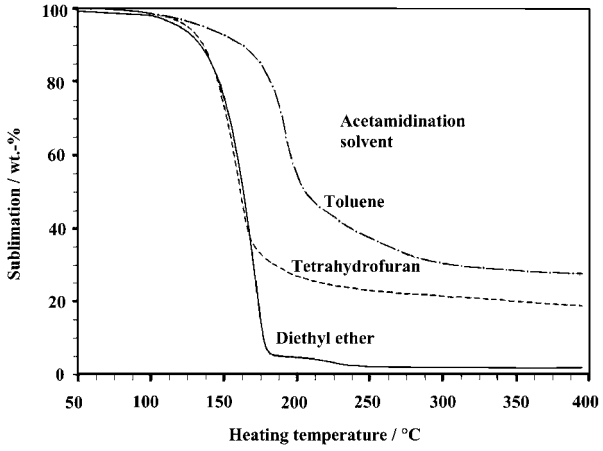

Figure 5. The effect of the amidination solvent on the sublimation of the iron(II) amidinate complex from iron(II) acetylacetonate at a heating rate of 10 °C/min.

Sublimation Kinetics of the Iron(II) Amidinates

A strong and regular effect of the heating rate on the nonisothermal TG and DTG curves of the iron(II) bis(*N*-*tert*-butyl-*N*′-ethylacetamidinate) obtained with iron(II) acetylacetonate as a starting iron(II) source in diethyl ether is shown in Figure 6. The isothermal TG and DTG curves of the iron(II) bis(*N*-*tert*-butyl-*N*′-ethylacetamidinate) obtained with iron(II) acetylacetonate and acetate as the starting iron(II) sources in diethyl ether are shown in Figure 7. According to Equations (1)–(3) of the Flynn–Wall technique the activation energy of sublimation for iron(II) bis(*N*-*tert*-butyl-*N*′-ethylacetamidinate)s and bis(*N*,*N*′-di-

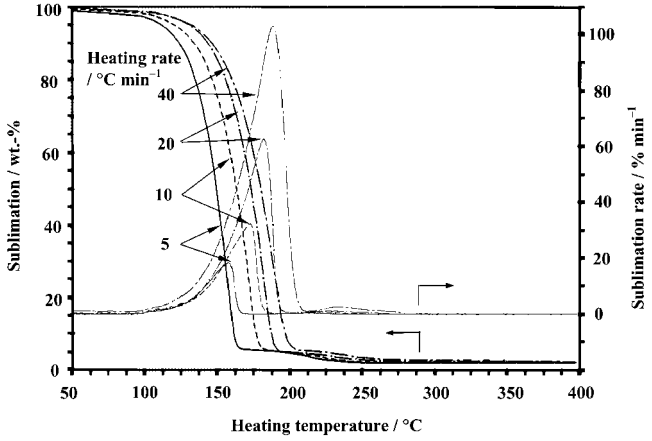

Figure 6. The effect of the heating rate on the the TG and DTG curves of the iron(II) bis(*N*-*tert*-butyl-*N*′-ethylacetamidinate) obtained with iron(II) acetylacetonate as a starting iron(II) source in diethyl ether.

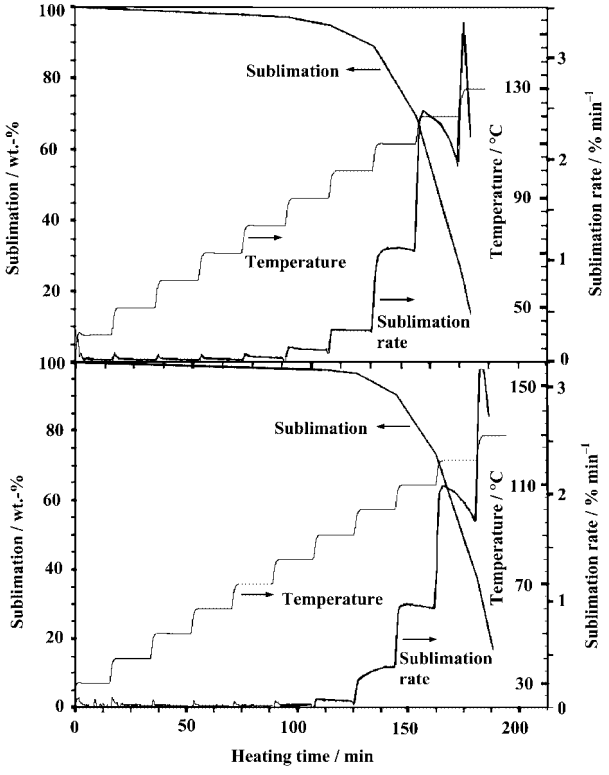

Figure 7. Multiple-stage isothermal TG and DTG curves of the iron(II) bis(*N*-*tert*-butyl-*N*′-ethylacetamidinate) obtained with iron(II) acetylacetonate (top) and iron(II) acetate (bottom) as starting iron(II) sources in diethyl ether.

isopropylacetamidinate) is summarized in Figure 8 and Table 2. Figure 8 discloses that the activation energy decreases with an increase in the sublimation level, indicating that a variation in the thermal sublimation kinetics, from diffusion-controlled kinetics to sublimation-controlled kinetics, is occurring. Under a large sample size at an early sublimation step the heat diffusion across the whole sample may be slow, leading to a diffusion control. As listed in Table 2, a larger sample size will result in a higher activation energy of the isothermal sublimation for sample No. **4**. It is also seen from Table 2 that two kinds of nonisothermal techniques, Flynn–Wall and Kissinger, afford similar activation energies of sublimation for the five iron(II) amidinates. However, the activation energy of the isothermal sublimation is different from that of the nonisothermal sublimation. In particular, the activation energy of the isothermal sublimation over a lower temperature range between 40 and 80 °C is much lower. In addition, the variation of the sublimation activation energy calculated by nonisothermal techniques for the iron(II) amidinates **1** to **7** is different from that calculated by isothermal techniques. These signify that the sublimation characteristics could vary with the heating method and temperature range. Nevertheless, it is interesting that the average activation energy (106 kJ mol^{-1}) for the nonisothermal sublimation at 127–198 °C is almost the same as the average activation energy (104 kJ mol^{-1}) determined from the isothermal thermogravimetric experiments at 80–130 °C.

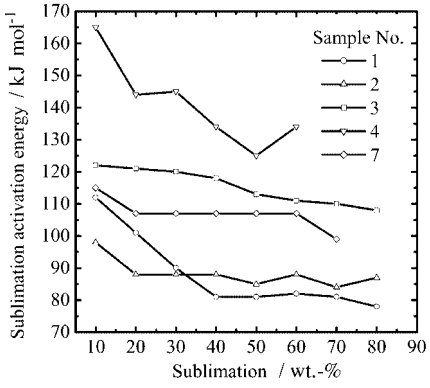

Figure 8. The variation of the sublimation activation energy with sublimation level based on the Flynn–Wall plot of ln (heating rate) against the reciprocal temperature for the iron(II) bis(*N*-*tert*-butyl-*N*′-ethylacetamidinate) and bis(*N*,*N*′-diisopropylacetamidinate).

Solubility and Solvatochromism of the Iron(II) Amidinates

All dark solid iron(II) amidinates will immediately become red upon exposure in air or water because of their fast decomposition over several seconds. That is to say, the iron(II) amidinates are highly air and moisture sensitive. Solubility of the iron(II) amidinates is investigated in several representative solvents with different dielectric constants in a nitrogen atmosphere. It is found that almost all the iron(II) bis(*N*-*tert*-butyl-*N*′-ethylacetamidinate)s and bis(*N*,*N*′-diisopropylacetamidinate) are readily soluble in most organic solvents like chloroform, benzene, pyridine, toluene, hexane, pentane, diethyl ether, and THF with dielectric constants between 1.9 and 13.3 but except for methanol with a high dielectric constant of 32.4. It is of interest that a variation of the amidinate solution color with the solvents is observed, i.e., a novel solvatochromism. The solution of the same amidinate exhibits different colors within various solvents. The black solid iron(II) bis(*N*-*tert*-butyl-*N*′-ethylacetamidinate) becomes blue in chloroform, purple in pyridine, and brown in benzene, toluene, hexane, pentane, diethyl ether, and THF. Similarly, dark-blue solid iron(II) bis(*N*,*N*′-diisopropylacetamidinate) becomes blue in chloroform, bluish black in benzene, and brown in pyridine. This indicates that the amidinate molecules may have different conformations and hence different solvates in different solvents, induced by the different interactions between the amidinate and the solvent molecules with different dielectric constants and polarity. In other words, the solvatochromism might be adjusted by changing the amidinate structure and choosing the solvent. However, there is no regular variation of the amidinate solvatochromism with the solvent dielectric constant. Similar solvatochromism has also been observed for the intrinsically conducting copolymers from orthanilic acid and aniline.[22]

Conclusions

A highly volatile and paramagnetic asymmetric iron(II) amidinate, iron(II) bis(*N*-*tert*-butyl-*N*′-ethylacetamidinate), was successfully synthesized. The optimal starting iron(II) compound and reaction solvent should be iron(II) acetylacetonate and diethyl ether, respectively, because the combination offers the highest yield, the strongest volatilizability of 98%, and the purest product. The NMR spectra of the iron(II) amidinates depend strongly on the deuterated sol-

Table 2. The activation energy (kJ mol^{-1}) of the sublimation of the iron bis(*N*-*tert*-butyl-*N*′-ethylacetamidinate) and bis(*N*,*N*′-diisopropylacetamidinate).

No.	Nonisothermal sublimation activation energy		Isothermal sublimation activation energy at a sample size of 2.1–3.0 mg	
	Flynn–Wall (average)	Kissinger	80–130 °C	40–80 °C
1	88	90	114	25
2	88	91	111	37
3	115	107	104	11
4	141	127	87(90)[a]	25(41)[a]
7	107	97	79	48

[a] The sample size is 3.9 mg.

vent used. It seems that deuterated chloroform is the optimal solvent for the structure characterization of the paramagnetic iron(II) amidinates. The different iron(II) amidinates from various starting iron(II) compounds exhibit almost the same NMR, MS, and IR spectra, a melting point of 85 °C (with an exception in THF around 25 °C), and solution color in the same solvents but different synthetic yields, paramagnetic fractions, volatilizabilities, and colors in different solvents. This implies that the iron(II) amidinates exhibit interesting variable paramagnetism and solvatochromism. The iron(II) bis(*N*-*tert*-butyl-*N*′-ethylacetamidinate) demonstrates an average activation energy of 106 kJ mol^{-1} for the nonisothermal sublimation, which is very close to the average activation energy of 104 kJ mol^{-1} calculated on the basis of the isothermal sublimation. The sublimation is a diffusion-controlled process because the temperature and rate of the sublimation depend strongly on the sublimation level and sample size. Great volatilizability at a lower temperature is a special feature of the asymmetric iron(II) amidinates compared with other related compounds.

Experimental Section

General: All reactions, manipulations, and characterizations were conducted under a nitrogen atmosphere using an inert atmosphere box. Tetrahydrofuran (THF), diethyl ether, toluene, and hexane were dried by using an innovative solvent purification system and stored over 0.4-nm molecular sieves. Methyllithium, 1-*tert*-butyl-3-ethyl-carbodiimide, 1,3-diisopropylcarbodiimide, anhydrous $FeCl_2$, iron(II) acetylacetonate[$Fe(CH_3COCH_2COCH_3)_2$], and iron(II) acetate (Aldrich) were used after vacuum treatment in nitrogen.

Iron(II) Bis(*N*-*tert*-butyl-*N*′-ethylacetamidinate) ([Fe(*t*Bu-Et-Me-AMD)$_2$]): A solution of methyllithium (1.6 M in diethyl ether, 3.8 mL, 6 mmol) in diethyl ether was added dropwise to a solution of 1-*tert*-butyl-3-ethyl-carbodiimide (0.9 g, 7 mmol) in diethyl ether (20 mL) at –30 °C. The mixture was warmed to room temperature and stirred for 4 h. This colorless mixture solution was then added to a solution of iron(II) acetylacetonate (0.9 g, 35 mmol) in diethyl ether (10 mL). The reaction mixture was stirred for 24 h. After all the volatiles were removed under reduced pressure the resulting solid was extracted with hexane (30 mL). The hexane extract was filtered through a pad of Celite on a glass frit to afford a dark solution. Subsequent sublimation afforded pure dark products (42%). Sublimation: 80 °C at 30 mTorr. The whole reaction procedure for the synthesis of the iron(II) complex is depicted in Scheme 1. The iron(II) bis(*N*,*N*′-diisopropylacetamidinate) was prepared in the same manner as described above. The iron(II) amidinate synthesized from iron(II) acetylacetonate in diethyl ether exhibits the following spectra: ^{1}H NMR ($CDCl_3$, 25 °C): 199.5 (broad, NCH_2CH$_3$), 56.7–111 (very broad, N_2CCH_3), 29.7 [broad, NC(CH_3)$_3$], –6.1 (sharp triplet, NCH_2CH_3) ppm for paramagnetic iron(II) amidinate; 8.6 (sharp, NCH_2CH$_3$), 3.5 (sharp, N_2CCH_3), 1.5 [broad, NC(CH_3)$_3$], 0.3 (sharp triplet, NCH_2CH_3) ppm for non-paramagnetic (diamagnetic) iron(II) amidinate. On the basis of the area ratio of the resonance peaks at 29.7 over 1.5 ppm it could be estimated that 55% of the product is paramagnetic. ^{1}H NMR (C_5D_5N, ([D$_5$]pyridine), 25 °C): 147.5 (sharp, NCH_2CH$_3$), 140.6 (sharp, N_2CCH_3), 9.1 (broad, NC(CH_3)$_3$), –15.9 (sharp, NCH_2CH_3) ppm for paramagnetic iron(II) amidinate; 4.7 (sharp, NCH_2CH$_3$), 2.8 (sharp, N_2CCH_3), 1.1 [broad, NC(CH_3)$_3$], 0.79 (sharp, NCH_2CH_3) ppm for diamagnetic iron(II) amidinate. The product could be 60% paramagnetic on the basis of the area ratio of the resonance peaks at 9.1 over 1.1 ppm. IR absorbances: 3268 (vw), 2968 (s), 2922 (s), 2854 (m), 1651 (vs), 1543 (m), 1457 (m), 1374 (m), 1288 (w), 1220 (m), 1157 (vw), 1031 (vw), 686 (s), and 548 (s) cm^{-1}. ES-MS at 120 °C: *m*/*z* [fragment, relative intensity (%)] = 331 [M – $(CH_3)_2$ + Na$^+$, 16], 321 [M – $(CH_3)_2$ + acetonitrile(MCN)$^+$, 7], 297 [M – $(CH_3)_2$–C_2H_5 + NH_4^+, 6], 269 [M – $(CH_3)_2$–$C(CH_3)_3$ + NH_4^+, 42], 207 [$FeNC(CH_3)NC(CH_3)_3$ + K$^+$, 6], 143 [$C_2H_5NC(CH_3)NC(CH_3)_3$ + 2H$^+$, 100]. The iron(II) amidinate from iron(II) acetate displays the following ^{1}H NMR ($CDCl_3$, 25 °C): 196.8 (broad, NCH_2CH$_3$), 56.3–114.5 (very broad, N_2CCH_3), 29.4 [broad, NC(CH_3)$_3$], –5.6 (sharp, NCH_2CH_3) ppm for paramagnetic iron(II) amidinate; 8.8 (sharp, NCH_2CH$_3$), 3.6 (sharp, N_2CCH_3), 1.2 [broad, NC(CH_3)$_3$], 0.4 (broad, NCH_2CH_3) ppm for diamagnetic iron(II) amidinate. On the basis of the area ratio of the resonance peaks at 29.4 over 1.2 ppm it could be calculated that 60% of the product should be paramagnetic. IR absorbances: 3250 (vw), 3043 (vw), 2962 (s), 2922 (s), 2856 (m), 1653 (vs), 1559 (m), 1510 (m), 1457 (m), 1374 (m), 1288 (w), 1220 (m), 1157 (vw), 1030 (vw), 687 (s), and 548(s) cm^{-1}. ES-MS at 120 °C: *m*/*z* [fragment, relative intensity (%)] = 350[M – C_2H_5 + MCN$^+$, 4], 331 [M – $(CH_3)_2$ + Na$^+$, 21], 321[M – $(CH_3)_2$ + MCN$^+$, 9], 281 [M – $C(CH_3)_3$, 4], 269 [M – $(CH_3)_2$–$C(CH_3)_3$ + NH_4^+, 8], 143 [$C_2H_5NC(CH_3)NC(CH_3)_3$] + 2H$^+$, 100]. The iron(II) amidinate synthesized from $FeCl_2$ in diethyl ether demonstrates the following: ^{1}H NMR ($CDCl_3$, 25 °C): 196.8 (broad, NCH_2CH$_3$), 56.3–115 (very broad, N_2CCH_3), 29.8 [broad, NC(CH_3)$_3$], –5.8 (sharp, NCH_2CH_3) ppm for paramagnetic iron(II) amidinate; 8.8 (sharp, NCH_2CH$_3$), 3.6 (sharp, N_2CCH_3), 1.4 [broad, NC(CH_3)$_3$], 0.6 (broad, NCH_2CH_3) ppm for diamagnetic iron(II) amidinate. It is evaluated based on the area ratio of the resonance peaks at 29.8 over 1.4 ppm that 58% of the product could be paramagnetic. ES-MS at 120 °C: *m*/*z* [fragment, relative intensity (%)] = 350 [M – C_2H_5 + MCN$^+$, 50], 349 [M – C_2H_5 + H$^+$ + K$^+$, 25], 348 [M – $(CH_3)_2$ + H$^+$ + K$^+$, 100], 339 [M + H$^+$, 16], 338 [M, 55], 331 [M – $(CH_3)_2$ + Na$^+$, 13], 324 [M – CH_3 + H$^+$, 17], 323 [M – CH_3, 87], 322 [M – $(C_2H_5)_2$ + MCN$^+$, 53]. The iron(II) amidinate synthesized from iron(II) acetylacetonate in toluene shows the following: ^{1}H NMR ($CDCl_3$, 25 °C): 56 (NCH_2CH$_3$), 29.2 (broad, N_2CCH_3), 16.2 [broad, NC(CH_3)$_3$], –5.8 (sharp, NCH_2CH_3) ppm for paramagnetic iron(II) amidinate; 8.6 (NCH_2CH$_3$), 3.2 (sharp, N_2CCH_3), 1.4 [broad, NC(CH_3)$_3$], 1.1 (broad, NCH_2CH_3) ppm for diamagnetic iron(II) amidinate. The paramagnetic fraction calculated based on the area ratio of the resonance peaks at 16.2 over 1.4 ppm is 37%.

Measurements: ^{1}H NMR spectra of the iron(II) amidinate solutions in test tubes filled with nitrogen were recorded with a Bruker AM-500 spectrometer. Melting points were obtained in a sealed capillary using optical microscopy. Infrared spectra were obtained with a Nicolet FT-IR 7000 spectrometer with sample solutions in diethyl ether in a nitrogen atmosphere. Mass spectra of the sample in THF were recorded with a Micromass LCT time-of-flight Mass Spectrometer operating in electrospray mode. Solution samples of the respective complexes in diethyl ether or THF were rapidly introduced by a direct inlet technique with acetonitrile as a mobile phase at a source temperature of 120–300 °C. Thermogravimetry (TG) was performed with a TGA Q50 V6.2 Build 187 thermogravimetric analyzer. Conventional constant heating-rate TG measurements were run at 5 °C, 10 °C, 20 °C, and 40 °C min^{-1} in nitrogen with a sample size of 1–3 mg to provide a control set of values for thermal sublimation parameters. Isothermally programmed TG analyses

were carried out at 40, 50, 60, 70, 80, 90, 100, 110, 120, and 130 °C in nitrogen at a flow rate of 40 mL min^{-1} with a sample size of 2–3 mg. The furnace was quickly heated at a heating rate of 60 °C min^{-1} to the selected temperature after the sample was inserted in the furnace. There are several techniques for the kinetic evaluation of the TG thermal weight-loss data, and they have been discussed in an earlier publication.[23] The thermal sublimation kinetics were examined by the following three evaluating techniques [Equation (1)], [Equation (2)], and [Equation (3)].

Flynn–Wall Technique[24]

$$\ln(\text{Heating rate}) = \ln(ZE/R) - \ln[F(a)] - E/(RT) \quad (1)$$

$$\ln(\text{Heating rate}/T_{sm}^2) = \ln[n(1-\alpha_m)^{n-1}ZR/E] - E/(RT_{sm}) \quad (2)$$

$$\ln(d\alpha/dt)_m = \ln Z + n\ln(1-\alpha_m) - E/(RT) \quad (3)$$

The activation energy, E, can be calculated from a plot of ln (heating rate) against $1/T$ (absolute temperature) at a fixed weight loss since the slope of such a line is given by E/R (gas constant 8.314 J mol^{-1}K^{-1}).

Kissinger Technique[25]

Where T_{sm} and α_m are the absolute temperature and sublimation, respectively, at the maximum sublimation rate $(d\alpha/dt)_m$. The slope of ln (Heating rate/T_{sm}^2) vs. $1/T_{sm}$ is equal to $-E/R$.

For an Isothermal TG Measurement at Several Isothermal Temperatures[23]

The E value of isothermal degradation was calculated from the slope of the plot of the maximum weight-loss rate ln $(d\alpha/dt)_m$ vs. the reciprocals of the several isothermal temperatures ($1/T$).

Acknowledgments

This work was supported in part by the National Science Foundation (grant ECS-0354213). We thank Leonard N. J. Rodriguez, Dr. Venkateswara Rao Pallem, Dr. Jin-Seong Park, and Dawen Pang from Harvard University, as well as Prof. Dr. Charles Musgrave from Stanford University for their valuable help.

[1] A. R. Sadique, M. J. Heeg, C. H. Winter, *J. Am. Chem. Soc.* **2003**, *125*, 7774–7775.
[2] J. R. Hagadorn, J. Arnold, *Angew. Chem. Int. Ed.* **1998**, *37*, 1729–1731; *Angew. Chem.* **1998**, *110*, 1813–1815.
[3] H. Kondo, K. Matsubara, H. Nagashima, *J. Am. Chem. Soc.* **2002**, *124*, 534–535.
[4] X. Jiang, J. C. Bollinger, M. H. Baik, D. Lee, *Chem. Commun.* **2005**, *8*, 1043–1045.
[5] J. Barker, N. C. Blacker, P. R. Phillips, N. W. Alcock, W. Errington, M. G. H. Wallbridge, *J. Chem. Soc., Dalton Trans.* **1996**, 431–437.
[6] D. Abeysekera, K. N. Robertson, T. S. Cameron, J. A. C. Clyburne, *Organometallics* **2001**, *20*, 5532–5536.
[7] C. Villiers, P. Thuery, M. Ephritikhine, *Eur. J. Inorg. Chem.* **2004**, *23*, 4624–4632.
[8] D. A. Kissounko, Y. H. Zhang, M. B. Harney, L. R. Sita, *Adv. Synth. Catal.* **2005**, *347*, 426–432.
[9] T. Chivers, C. Fedorchuk, M. Parvez, *Organometallics* **2005**, *24*, 580–586.
[10] B. S. Lim, A. Rahtu, J.-S. Park, R. G. Gordon, *Inorg. Chem.* **2003**, *42*, 7951–7958.
[11] a) D. Hausmann, J. Becker, S. Wang, R. G. Gordon, *Science* **2002**, *298*, 402–406; b) B. S. Lim, A. Rahtu, R. G. Gordon, *Nat. Mater.* **2003**, *2*, 749–754; c) R. G. Gordon, S. Barry, R. N. R. Broomhall-Dillard, D. J. Teff, *Adv. Mater. Optics Electron.* **2000**, *10*, 201–211.
[12] A. I. Kingon, J. P. Maria, S. K. Streiffer, *Nature* **2000**, *406*, 1032–1038.
[13] Z. Li, S. T. Barry, R. G. Gordon, *Inorg. Chem.* **2005**, *44*, 1728–1735.
[14] F. T. Edelmann, D. M. M. Freckmann, H. Schumann, *Chem. Rev.* **2002**, *102*, 1851–1896.
[15] H. E. Abdou, A. A. Mohamed, J. M. Lopez-de-Luzuriaga, J. P. Fackler, *J. Cluster Sci.* **2004**, *15*, 397–411.
[16] a) R. T. Boere, M. L. Cole, P. C. Junk, *New J. Chem.* **2005**, *29*, 128–134; b) F. A. Cotton, N. S. Dalal, C. Y. Liu, C. A. Murillo, J. M. North, X. P. Wang, *J. Am. Chem. Soc.* **2003**, *125*, 12945–12952.
[17] a) M. J. McNevin, J. R. Hagadorn, *Inorg. Chem.* **2004**, *43*, 8547–8554; b) P. de Rouffignac, J. S. Park, R. G. Gordon, *Chem. Mater.* **2005**, *17*, 4808–4814; c) W. X. Zhang, M. Nishiura, Z. M. Hou, *J. Am. Chem. Soc.* **2005**, *127*, 16788–16789; d) M. L. Cole, C. Jones, P. C. Junk, M. Kloth, A. Stasch, *Chem. Eur. J.* **2005**, *11*, 4482–4491.
[18] H. Kawaguchi, T. Matsuo, *Chem. Commun.* **2002**, *9*, 958–959.
[19] B. Vendemiati, G. Prini, A. Meetsma, B. Hessen, J. H. Teuben, O. Traverso, *Eur. J. Inorg. Chem.* **2001**, *3*, 707–711.
[20] J. Zhang, R. Ruan, Z. Shao, R. Cai, L. Weng, X. Zhou, *Organometallics* **2002**, *21*, 1420–1424.
[21] a) B. Clare, N. Sarker, R. Shoemaker, J. R. Hagadorn, *Inorg. Chem.* **2004**, *43*, 1159–1166; b) V. K. K. Praneeth, C. Näther, G. Peters, N. Lehnert, *Inorg. Chem.* **2006**, *45*, 2795–2811.
[22] X.-G. Li, R.-R. Zhang, M.-R. Huang, *J. Comb. Chem.* **2006**, *8*, 174–183.
[23] X.-G. Li, M.-R. Huang, *Polym. Degrad. Stabil.* **1999**, *64*, 81–90.
[24] J. H. Flynn, L. A. Wall, *J. Polym. Sci. B* **1966**, *4*, 323–328.
[25] H. E. Kissinger, *Anal. Chem.* **1957**, *29*, 1702–1706.

Received: August 18, 2006
Published Online: February 9, 2007

